On pathloss models for adjacent-channel interference in cognitive whitespace systems

Andreas F. Molisch, *Fellow, IEEE,* Zaid Hijaz, *Member, IEEE,* William J. Nunan, and Laurence F. Zapanta

***Abstract*—Adjacent channel interference is one of the fundamental processes limiting wireless system performance. In particular, cognitive radio exploiting "whitespace," i.e., spectral guard bands between existing services, are limited by adjacent channel interference to victim receivers. Upper-bounding such interference requires accurate knowledge of minimum pathloss at short range (less than a few hundred meters), but existing, standardized models focus on maximum pathloss at long range. This paper discusses methods to characterize more accurately the low pathloss regime. These improved models account for variations of the pathloss exponents, the random nature of the occurrence of line-of-sight, and the distance dependence of fading parameters. By comparing standard models to ray tracing results, we demonstrate the large impact that such modeling considerations can have on outage probability in cognitive systems.**

***Index Terms*—Propagation channel, pathloss, adjacent-channel interference, whitespace, secondary users.**

I. Introduction

The proliferation of wireless services demands more efficient use of spectral resources. One improvement is the reduction of guard bands between existing services, and another is the use of such "white space" (i.e. those guard bands) for new services [1]. The most prominent example is the white space between TV channels, but other spectrum sharing opportunities exist as well. In order to assess the resulting interference to primary services, one must adopt realistic propagation models, since the propagation channel (in conjunction with the transmit power of the new services) determines the received interference.

Propagation channel models for cognitive radio have received a lot of attention (see, e.g., [2], and references therein). Classical cognitive radio systems operate on the same frequency as the primary (victim) receiver, and therefore present a risk of *co-channel interference*. In order to avoid such interference, the secondary transmitter either does not transmit while a primary signal is on the air, or by design the secondary transmitter is much farther away than the primary transmitter from the primary (victim) receiver. In contrast, white space systems operate concurrently with and in close proximity to primary receivers, creating *adjacent channel interference* (ACI) that is attenuated by the transmit/receive filter combination[1].

At first glance the two situations might seem equivalent, since the performance of the primary system is impacted only by the *level* of interference arriving at the detector, and not how it was created (i.e., co-channel or adjacent-channel). However most (outdoor) channel models are optimized to reflect the channel characteristics at medium to large distances (near the cell edge for cellular systems), where the received signal is weakest. Similarly most experimental verification of channel models emphasizes only the correct description of fading dips. The analysis of whitespace interference must also address the peaks in the fading distributions, and pathloss accuracy at *short distances*, where attenuation is much lower. Fading dips and maximum pathloss are most important for coverage analysis; however, for whitespace interference analysis the power peaks and minimum pathloss are paramount.

For all these reasons, it is important to investigate how established, standardized propagation models fare when used for the computation of adjacent-channel interference induced outage. While this discussion concentrates on cognitive whitespace systems, the same pathloss analysis is applicable to *any* wireless system impacted by adjacent-channel interference. The current paper provides such an analysis based on fundamental physics, established literature, and simulations with a ray tracer that has been calibrated with measurements. The main conclusion from our investigation is that in such systems (i) standardized pathloss models can show significant deviations from the pathloss in a particular area (e.g., a specific city), (ii) the pathloss coefficient and shadowing variance should be treated as random variables, (iii) it is advantageous to use a probabilistic model for the occurrence of line-of-sight (LOS) situations, (iv) the distance dependence of fading parameters such as the shadowing variance must be taken into account. Failure to incorporate these effects can lead to misestimation of adjacent channel interference levels and resulting outage probabilities.

The remainder of this paper is organized as follows: Section II describes the fundamental propagation effects and their representation in standardized pathloss models. Section III outlines modifications that are required for the situation of interest. Section IV presents example results based on ray tracing in urban and suburban environments. A summary and conclusions are given in Sec. V.

A. F. Molisch is with the University of Southern California, Ming-Hsieh Department of Electrical Engineering, Los Angeles, California 90089, (e-mail: molisch@usc.edu.)

Zaid Hijaz, William Nunan, and Laurence Zapanta are with the Aerospace Corporation, Los Angeles, California 90245 (e-mail: {zaid.hijaz, william.j.nunan, laurence.f.zapanta}@aero.org.

[1]In such cases the level of adjacent channel interference depends on how well the secondary system confines its emissions, and also how well the primary receiver rejects out-of-band signals – a feature that the secondary system cannot control.

II. Standardized Channel Models

A. Deterministic models

Channel models generally fall into one of two categories: deterministic or stochastic. Deterministic models use a numerical approximation to Maxwell's equations (e.g., a ray tracing approach) in conjunction with a database that specifies the boundary conditions in the area of interest, such as building geometry, dielectric properties of building materials, terrain data map, etc. This approach provides the received power, impulse responses and directional characteristics for a given environment. Several investigations have quantified the difference between measured received powers and predictions based on ray tracing. Typically, the narrowband power (averaged over the small-scale fading) is predicted with a mean error and a standard deviation of 6 dB [3]–[7], with the errors approximated as Gaussian. In Section IV, we will discuss more detailed comparisons for a commercial ray tracer, Wireless InSite [8], which has been compared against extensive measurements. Calibrating ray tracing results (with respect to measurements) and assessing their reliability is important because ray tracing allows evaluation of a larger number of samples and a larger variety of system parameters than can be achieved in measurement campaigns.

B. Generic stochastic models

The local (instantaneous) channel gain is usually modeled as the product of three factors: (i) the distance-dependent path gain, (ii) a random variable representing shadowing S, which is typically log normally distributed, with standard deviation σ_{S}, and (iii) a random variable representing small-scale fading, whose amplitude is often modeled as gamma-distributed, representing a Nakagami amplitude distribution. In the absence of a line-of-sight (LOS) between transmitter and receiver, this variable is often modeled as Rayleigh distributed. Since the small-scale fading is often averaged out through frequency diversity in wideband systems, and antenna diversity in MIMO systems, we will not consider it further here.

The pathloss (inverse of the path gain) is usual modeled, on a dB scale, as

$$PL_{\mathrm{dB}} = \alpha + 10n\log(d/d_0) \tag{1}$$

where d_0 is the reference distance, and α and n are constants obtained either from physical considerations, or from fitting to measurement/ray tracing results.

C. Breakpoint models and probabilistic pathloss models

A more sophisticated pathloss model does not use a single straight-line fit, since pathloss tends to increase nonlinearly as a function of $log(d)$. In practice, this increase is mainly due to the fact that as the distance increases, the probability decreases that the receiver has LOS to the transmitter [9]. Since non-LOS (NLOS) leads to higher pathloss (smaller path gain), this leads to an increase in the slope. The effect is typically modeled in one of two ways: A breakpoint model [10] describes the pathloss as follows:

$$PL_{\mathrm{dB}} = \begin{cases} \alpha + 10n_1\log(d/d_0) & \text{for} \quad d < d_{\mathrm{break}} \\ \alpha + 10n_1\log(d_{\mathrm{break}}/d_0) & \\ \quad + 10n_2\log(d/d_{\mathrm{break}}) & \text{elsewhere} \end{cases} \tag{2}$$

This model makes no explicit distinction between LOS and NLOS, but the breakpoint often arises due to the transition from LOS to NLOS.

Alternatively, one can express both LOS and NLOS pathloss in the form of Eq. (1), but with different parameters α and n for the two regimes. The probability that a clear LOS exists from transmitter to receiver is denoted $p_{\mathrm{LOS}}(d)$, which typically decreases with distance. For system simulations, receiver locations are chosen to be in LOS or not according to a specified random distribution, and then the corresponding LOS or the NLOS pathloss model is used.

We note that in addition to the LOS/NLOS transition, there are also other effects that can increase the slope with increasing distance:

- In a pure LOS propagation over plane earth, the destructive interference between the direct and reflected rays leads to a transition from d^2 to d^4 dependence for distances larger than a breakpoint $d_{\mathrm{break}} = 4h_{\mathrm{Tx}}h_{\mathrm{Rx}}/\lambda$, where λ is the wavelength [10].
- Even the slope in NLOS propagation might increase as the distance increases (see [11] and references therein). This occurs because more efficient propagation processes such as wave guiding through street canyons become unavailable at larger distances (e.g. when the canyons are not long enough), or when the receiver moves beyond the radio horizon.

These effects can be accommodated in the probabilistic LOS model by using separate breakpoint models for LOS and NLOS. For our chosen environment and system parameters, such a generalization did not provide meaningful improvement of accuracy, and will thus not be further considered; however it could be relevant for other settings.

D. Standardized models

A number of commonly used standardized models follow the above approach. For macrocells, pure power pathloss models of type (1) have been used, e.g., in the well-known Okamura-Hata model, which describes the dependence of the parameters α and n on frequency, base station (BS) and mobile station (MS) heights, and environment. COST 231 extends this model's frequency range up to 1500 MHz [4]. However, the Hata models are applicable only for distances $d > 1$ km, and thus are not valid for analyzing interference that a BS causes to other systems much closer than 1 km, as is relevant for ACI modeling.

For distances between 20 m and 5 km, the COST 231 Walfish Ikegami model [4] proposes a simple fit according to (1) for LOS situations, with $d_0 = 20$ m, α as the free-space pathloss at d_0, and $n = 2.6$ [2]. The pathloss coefficient

[2]The COST 231 model for NLOS is much more complicated, and depends on building height, street width, and street orientation

of 2.6 is higher than the free-space value of 2, which is peculiar for LOS situations. Typically $n < 2$ in street canyon environments, due to wave guiding effect, as we will also show in Sec. IV. Note that the COST 231 models are also used as the pathloss models in the 3GPP Spatial Channel Model [12].

The Winner/ITU R models also use separate LOS and NLOS power laws as described above (1), and furthermore provide a distance-dependent probability for having LOS [9]. These models tend to have rather high pathloss coefficients for LOS situations.

In addition to these models, a variety of others exist, most notably the COST 259 model [13], and several ITU (International Telecommunications Union) models. The listing here is thus intended to provide only a few representative examples. Reference [14] gives a more extensive survey.

III. Modifications for whitespace systems

In this section we describe channel model modifications that are especially relevant to whitespace systems. Channel models generally are independent of the particular application, but any channel model makes simplifications. The most common simplifications are made to ensure adequate service for an MS far from the BS. Upper bounding the interference to whitespace systems demands that we focus on modeling aspects that are frequently neglected in order to assess the probability of outages created by interferers close to the victim receiver.

A. Fitting methods for short distances

Pathloss modeling consists of computing a "best fit" of a parameterized curve of certain shape (typically a line on a log-log plot) to a set of measurements. Such curve fits are heavily influenced by the density of measurement points at different distances[3]. Most measurement campaigns collect more points at larger distances, because these are more important for computing coverage in traditional cellular systems. Such models - dominated by distant points - may contain large errors in the region close to the transmitter, and therefore may be highly inaccurate for the analysis of interference to whitespace systems.

Over-weighting larger distances in the curve fit can cause an over- or underestimation of the pathloss at small distances. When a concave-up function (like the combined LOS and NLOS pathloss described in Sec. II-C) is fitted by a straight line, that line falls below the data points at short distances, leading to an underestimation of the data.

Similarly a straight line fit to a concave-down function overestimates the actual pathloss at short distances. This can occur, e.g., when only LOS measurements are analyzed. At extremely short distances, the pathloss is essentially given by the $n = 2$ free-space pathloss (after averaging out small-scale fading created, e.g., by the interference from ground reflections). As the distance increases, the power from the reflections from nearby objects is added, so that the pathloss is less than the free-space value, and a straight-line fit underestimates the received power[4].

We wish to point out the common misconception that pathloss values smaller than free-space are unphysical. In fact reflections can add constructively to the direct ray to increase the received power. This effect leads to the frequently observed $n < 2$ in LOS situations.

B. Distance dependence of fading parameters

The shadowing variance is commonly modeled as distance-indepenent, to reduce the number of parameters that need to be fitted. In reality, the variance tends to increase with distance. The distance-independent model leads to an overestimation of the variance at short distances. We therefore anticipate that the shadow-induced variations may be smaller than standardized model predictions, thus somewhat counteracting the effect of stochastic pathloss coefficient variations described below.

C. Stochastic modeling of the pathloss coefficient

The standard pathloss coefficient is usually obtained by taking the expectation over all directions from the BS, as well as over multiple BS locations. However, work in [16]–[18] showed that pathloss coefficients in different cells can be different even when the cells are in the same type of environment; therefore, they should be modeled as random variables. Treating n and σ_{S} as random variables has important implications for whitespace systems. In order to achieve low outage probabilities at the receiver, the transmitter must provide sufficient margin to accommodate the increased variability of the interference power received by the victim. Any increase in this margin correspondingly increases the stand-off distance between transmitter and receiver.

IV. Simulations results

In this section we show ray tracing results to demonstrate and quantify the above-mentioned phenomena. We will show mainly two types of results: pathloss/shadowing and "outage". In the context of the aforementioned whitespace system, an outage occurs if the pathloss (including shadowing) at a particular location falls below a threshold T. That threshold represent the minimum required attenuation of an adjacent-channel interferer such that the victim receiver can still operate. Since this value depends on the specific system being considered, we will show families of curves for different values of T.

A. Ray tracing setup

Fig. 1 is a map of the Tx and Rx locations in a representative urban environment - Ottawa, Canada - used in our ray tracing simulations. The area is characterized by wide boulevards and several open places.

We selected 16 different Tx positions, as well as a large number of Rx positions, providing overall more than 100,000

[3] This issue could be mitigated through appropriate weighting [15]; however, to the best of the authors' knowledge such weighting has not been done in the establishment of standardized channel models.

[4] Note that beyond the breakpoint, the pathloss coefficient increases, as discussed in Sec. II.C

Fig. 1. Simulation environment in Ottawa, Canada.

Tx-Rx combinations. We did similarly extensive simulations in a suburban environment, Rosslyn, VA, USA. The map is not shown here for space reasons.

The ray tracing simulations were done with a commercial ray tracer, Wireless InSite, by Remcom [8]. This specific ray tracer is widely used, and has been compared to measurements in a number of papers, e.g., [19]. Due to this experimental verification in a variety of environments, one can have reasonable confidence that the ray tracer results are representative of physical reality in the specific locations being modeled.

B. Fundamental effects

Fig. 2 shows an example scatter plot of the pathloss obtained with respect to one particular Tx position in Ottawa. From this example we can draw a number of important conclusions:

- The shadowing standard deviation increases significantly with distance, especially for NLOS, but also for LOS. If one were to use the standard model in which the (shadowing) standard deviation is computed as the mean of the deviations of any measurement point from the linear regression, then the shadowing would be over-estimated at short distances and under-estimated at long distances. This is further demonstrated in Fig. 3, which also shows that a linear increase (with $log(d)$) is a good approximation. This change in the standard deviation might not be purely due to shadowing in the conventional sense, but rather to a greater variety of surroundings near the Rx points. Even if Rx locations are uniformly distributed, there are more Rx points at larger distances, and thus a greater variety of environments around the Rxs.
- Free-space pathloss is *not* a worst-case with respect to adjacent-channel interference. Rather pathloss less than free-space (leading to worse interference) can be observed in a large percentage of cases. Furthermore, the Hata model for the urban scenario tends to overestimate the pathloss significantly.
- Fitting of the ray tracing results (or measurements) to all points gives wrong results for certain distance ranges. Fig. 2 shows the best straight-line fit for NLOS when all points are weighed equally. Since most NLOS evaluation points are at large distances, those distance regions are fitted best. For small distances, e.g., 30 m, the straight-line fit overestimates the pathloss by about 10 dB. We stress that the fit need not *over*estimate pathloss in all cases; for other simulation points we observed an underestimation as well (not shown here for space reasons).

We next demonstrate that a model of type (1) combined with a *distance-dependent* lognormal shadowing can well represent the statistical behavior of the channel *associated with one*

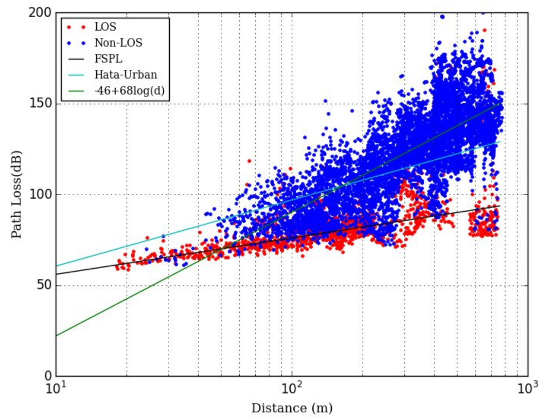

Fig. 2. Scatter plot of pathloss obtained from ray tracing in Ottawa, Canada, for Tx position 13. LOS points are in red, NLOS points in blue. The line $= 46 + 68log(d)$ is the best line fit to the NLOS data. FSPL is free space pathloss.

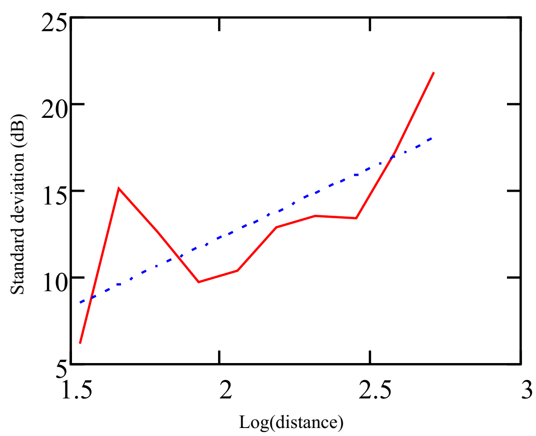

Fig. 3. Shadowing standard deviation, as a function of distance, for Tx position 14 in Ottawa.

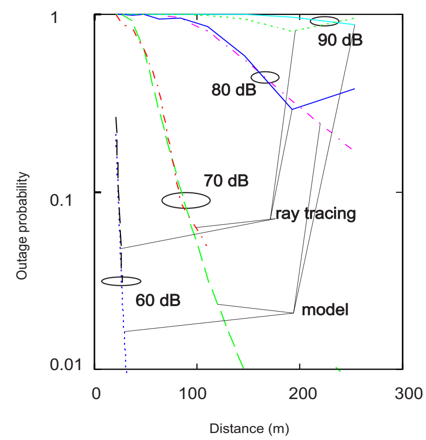

Fig. 4. Outage probability in LOS for Tx position 3 in Rosslyn (suburban) obtained directly from ray tracing data, and from power-law+shadowing model.

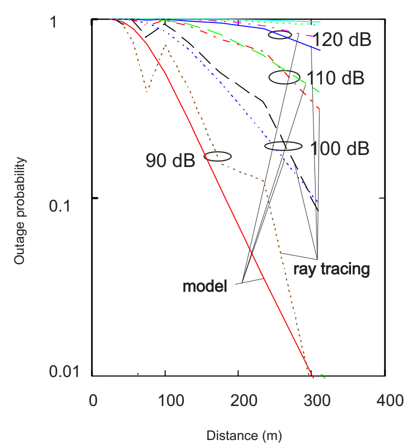

Fig. 5. Outage probability in NLOS for Tx position 3 in Rosslyn (suburban) obtained directly from ray tracing data, and from power-law+shadowing model.

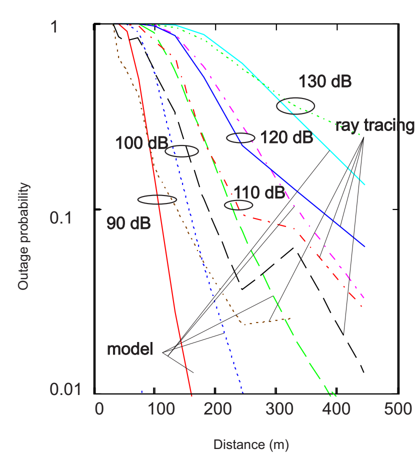

Fig. 6. Outage probability in NLOS for Tx position 14 in Ottawa (urban) obtained directly from ray tracing data, and from power-law+shadowing model.

BS in a suburban environment, if the model parameters are fitted to the specific environment. Figs. 4 and 5 show the outage probability in LOS and NLOS situations, respectively, for one particular Tx location in Rosslyn. The figures show the outage probability as computed directly from the ray tracing results, and also as computed from a model. We see very good agreement, but some deviations are to be expected due to the limited number of simulation points. Similar results were obtained for the other Tx positions in Rosslyn. The agreement is not quite as good in the investigated urban environment; see Fig. 6. The disagreement is even more pronounced at LOS situations (not shown here for space reasons). Still, for clarity of exposition (using smooth curves), we henceforth mostly use such "per BS" fitted models to represent our results.

C. Random pathloss coefficient

We next demonstrate the importance of variations of the pathloss coefficients associated with different BSs. Fig. 7 shows the outage curves for a $T = 80$ dB for the different BSs, Tx 1 to Tx 9. We see that the admissible BS-MS distances

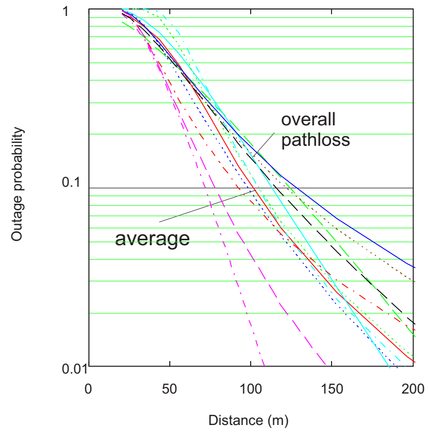

Fig. 7. Outage probability in NLOS for a 80 dB threshold in Ottawa, for 9 sample Tx positions. Red line: outage averaged over all (16) different Tx positions). Black dashed curve: outage probability computed from a pathloss and shadowing fit to all ray tracing data.

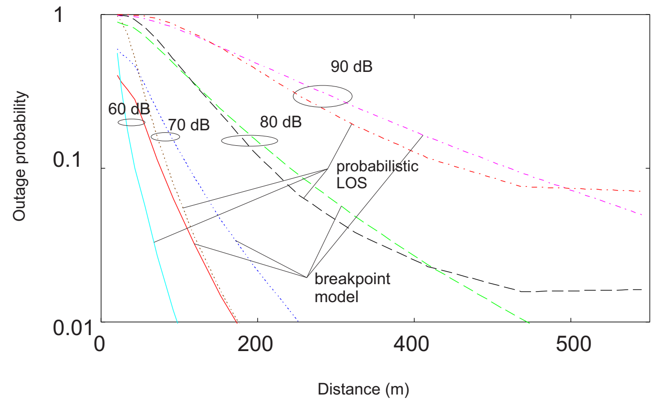

Fig. 8. Outage probability as a function of distance, averaged over all Tx, for breakpoint model and probabilistic LOS model, in Ottawa.

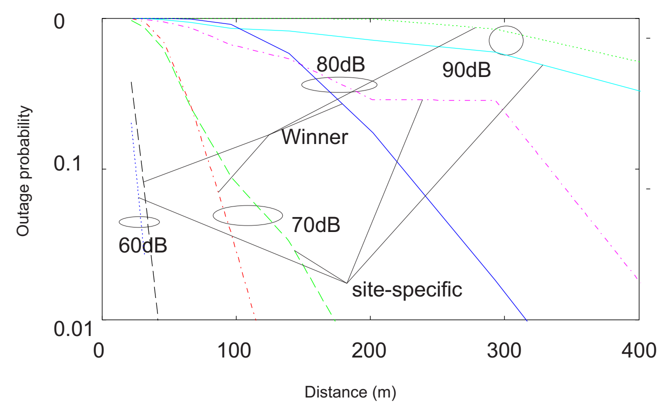

Fig. 9. Comparison of outage probability compared with the Winner model versus site-specific evaluation.

can vary drastically, especially at low outage probabilities. For example, given a 5% outage probability, the corresponding distance to the victim receiver could be as small as 100 m, or as large as 180 m. Clearly system planning based on only averages would not properly account for the fact that some regions may be much more strongly impacted. In addition, proper system design must take account of different possible definitions for average outage probability. One may compute the outage probability separately for each Tx position, and then average over all Tx positions. Alternatively one may first fit a power law model (including distance dependent shadowing) to all ray tracing data, and use the resulting model to obtain the overall outage probability. While the difference is not very large, it may be significant, as can be seen comparing the red and black curves in Fig. 7.

D. Probabilistic LOS model versus breakpoint model

We next compare methods for incorporating both LOS and NLOS situations. Sec. II discussed both the breakpoint model and the model based on separate LOS and NLOS power-law models that are combined based on the probability of LOS occurrence. Fig. 8 compares the results. The two methods agree reasonably for large outage probabilities, but diverge for small probabilities.

E. Comparison to standardized systems

Standardized models allow comparison of different systems under reproducible channel states; however, ray tracing results (and models derived from them) are much better site-specific representations of the channels. Fig. 9 compares the outage probability for LOS situations with those directly obtained from the ray tracing results. At small distances, there is reasonable agreement, in the sense that the distances at which a certain outage level is achieved are within 20% of each other. This occurs because the Winner model is very close to the free-space pathloss at short distances. Even though a considerable percentage of measurement points have pathloss smaller than free-space (as discussed above), the standard deviation of pathloss is small at short distances, so that the outage-vs-distance curves have steep slopes. Therefore, the difference between the ray tracing and Winner *distances* at a fixed *outage probability* are small even though there are large differences between ray tracing and Winner *outage probabilities* at a fixed *distance*.

For larger distances (higher outage thresholds), the difference between Winner and ray tracing results increases dramatically. Not only the absolute values, but also the shapes, are quite different. This is all the more noteworthy as this comparison is for LOS, where models generally differ less than in NLOS situations. One cause of this discrepancy is Winner's use of $n = 2.2$, in contrast to ray tracing results in which n ranges from 1.7 to 1.9, as discussed in Sec. II. Furthermore, Winner does not model the distance dependence of the shadowing variance.

V. Conclusions

In this paper we investigated the impact of propagation channel models on the performance of wireless systems limited by adjacent-channel interference, of which "white space" cognitive radio systems are a very important example. Since conventional channel models are optimized for assessment of coverage by primary systems, they do not provide a sound basis for limiting worst case interference in the operation of white space systems. We found that (i) model parameters should be fitted for the distance range in which evaluations are to be performed; (ii) pathloss coefficient and shadowing standard deviation should be treated as random variables the values of which may depend significantly on the particular environment; (iii) probabilistic modeling of the occurrence of line-of-sight (LOS) situations is beneficial, though breakpoint models can provide reasonable results as well, and (iv) the distance dependence of fading parameters such as the shadowing standard deviation must be taken into account.

Most standardized channel models cannot be used with high confidence for assessment of whitespace systems. Even free-space pathloss does not define worst-case interference, since in LOS situations, the pathloss coefficient is often lower than $n = 2$; therefore, received interference power higher than simple free-space is common.

These results show that preventing excessive interference to victim receivers associated with whitespace systems can be assured only via site-specific modeling, or extremely conservative stochastic modeling. Propagation models designed for edge coverage can overstate the path loss for short distances, thereby increasing the likelihood that systems that share spectrum will interfere with one another.

Our analysis has concentrated on the interference from a single, dominant source. The computation of interference distributions arising from a multitude of sources is discussed, e.g., in [20]–[25].

References

[1] S. J. Shellhammer, A. K. Sadek, and W. Zhang, "Technical challenges for cognitive radio in the TV white space spectrum," in *Information Theory and Applications Workshop, 2009*. IEEE, 2009, pp. 323–333.

[2] A. F. Molisch, L. J. Greenstein, and M. Shafi, "Propagation issues for cognitive radio," *Proceedings of the IEEE*, vol. 97, no. 5, pp. 787–804, 2009.

[3] V. Erceg, S. J. Fortune, J. Ling, R. Valenzuela *et al.*, "Comparisons of a computer-based propagation prediction tool with experimental data collected in urban microcellular environments," *Selected Areas in Communications, IEEE Journal on*, vol. 15, no. 4, pp. 677–684, 1997.

[4] E. Damosso, "Digital mobile radio: COST-231 view on the evolution towards 3rd generation systems," *European Commission*, 1998.

[5] Z. Yun and M. F. Iskander, "Ray tracing for radio propagation modeling: Principles and applications," *Access, IEEE*, vol. 3, pp. 1089–1100, 2015.

[6] W. Zhang, "Fast two-dimensional diffraction modeling for site-specific propagation prediction in urban microcellular environments," *Vehicular Technology, IEEE Transactions on*, vol. 49, no. 2, pp. 428–436, 2000.

[7] S.-C. Kim, B. J. Guarino Jr, T. M. Willis III, V. Erceg, S. J. Fortune, R. Valenzuela, L. W. Thomas, J. Ling, J. D. Moore *et al.*, "Radio propagation measurements and prediction using three-dimensional ray tracing in urban environments at 908 MHz and 1.9 GHz," *Vehicular Technology, IEEE Transactions on*, vol. 48, no. 3, pp. 931–946, 1999.

[8] Remcom, "Wireless InSite: Wireless EM propagation software," 2015.

[9] P. Kyösti, J. Meinilä, L. Hentilä, X. Zhao, T. Jämsä, C. Schneider, M. Narandzić, M. Milojević, A. Hong, J. Ylitalo *et al.*, "Winner ii channel models," 2008.

[10] A. F. Molisch, *Wireless Communications, 2nd edition*. John Wiley & Sons, 2011.

[11] C. Galiotto, I. Gomez-Miguelez, N. Marchetti, and L. Doyle, "Effect of LOS/NLOS propagation on area spectral efficiency and energy efficiency of small-cells," in *Global Communications Conference (GLOBECOM), 2014 IEEE*. IEEE, 2014, pp. 3471–3476.

[12] G. Calcev, D. Chizhik, B. Göransson, S. Howard, H. Huang, A. Kogiantis, A. F. Molisch, A. L. Moustakas, D. Reed, and H. Xu, "A wideband spatial channel model for system-wide simulations," *Vehicular Technology, IEEE Transactions on*, vol. 56, no. 2, pp. 389–403, 2007.

[13] H. Asplund, A. A. Glazunov, A. F. Molisch, K. Pedersen, M. Steinbauer *et al.*, "The COST-259 directional channel model-part ii: macrocells," *Wireless Communications, IEEE Transactions on*, vol. 5, no. 12, pp. 3434–3450, 2006.

[14] C. Phillips, D. Sicker, and D. Grunwald, "A survey of wireless path loss prediction and coverage mapping methods," *Communications Surveys & Tutorials, IEEE*, vol. 15, no. 1, pp. 255–270, 2013.

[15] A. Karttunen *et al.*, "Impact of spatial measurement density on pathloss modeling," in *Proc. IEEE ICC*, 2016.

[16] V. Erceg, L. J. Greenstein, S. Y. Tjandra, S. R. Parkoff, A. Gupta, B. Kulic, A. Julius, R. Bianchi *et al.*, "An empirically based path loss model for wireless channels in suburban environments," *Selected Areas in Communications, IEEE Journal on*, vol. 17, no. 7, pp. 1205–1211, 1999.

[17] S. S. Ghassemzadeh, R. Jana, C. W. Rice, W. Turin, and V. Tarokh, "Measurement and modeling of an ultra-wide bandwidth indoor channel," *Communications, IEEE Transactions on*, vol. 52, no. 10, pp. 1786–1796, 2004.

[18] Z. Li, R. Wang, and A. F. Molisch, "Shadowing in urban environments with microcellular or peer-to-peer links," in *Antennas and Propagation (EUCAP), 2012 6th European Conference on*. IEEE, 2012, pp. 44–48.

[19] K. Rizk, J.-F. Wagen, and F. Gardiol, "Two-dimensional ray-tracing modeling for propagation prediction in microcellular environments," *Vehicular Technology, IEEE Transactions on*, vol. 46, no. 2, pp. 508–518, 1997.

[20] M. Z. Win, P. C. Pinto, L. Shepp *et al.*, "A mathematical theory of network interference and its applications," *Proceedings of the IEEE*, vol. 97, no. 2, pp. 205–230, 2009.

[21] A. Rabbachin, T. Q. Quek, H. Shin, and M. Z. Win, "Cognitive network interference," *Selected Areas in Communications, IEEE Journal on*, vol. 29, no. 2, pp. 480–493, 2011.

[22] P. Dmochowski, P. J. Smith, M. Shafi, J. G. Andrews, R. Mehta *et al.*, "Interference models for heterogenous sources," in *Communications (ICC), 2012 IEEE International Conference on*. IEEE, 2012, pp. 4049–4054.

[23] L. Vijayandran, P. Dharmawansa, T. Ekman, and C. Tellambura, "Analysis of aggregate interference and primary system performance in finite area cognitive radio networks," *Communications, IEEE Transactions on*, vol. 60, no. 7, pp. 1811–1822, 2012.

[24] S. Kusaladharma and C. Tellambura, "A multiple-ring model for cognitive radio aggregate interference," *Communications Letters, IEEE*, vol. 18, no. 4, pp. 596–599, 2014.

[25] M. S. Ali and N. B. Mehta, "Modeling time-varying aggregate interference in cognitive radio systems, and application to primary exclusive zone design," *Wireless Communications, IEEE Transactions on*, vol. 13, no. 1, pp. 429–439, 2014.